Electronic Supplementary Material (ESI) for Journal of Materials Chemistry A.
This journal is © The Royal Society of Chemistry 2023

Supporting Information

Crystal Transformation of Metal–Organic Framework to Boost Visible-Light Photocatalysis via Amine Adsorption

Xin Liu, Zhifen Guo, Yan Che, Mengying Li, Xingbing Liu, Fengchao Cui* and Hongzhu Xing*

College of Chemistry, Northeast Normal University, Changchun 130024, China.

E-mail: cuifc705@nenu.edu.cn; xinghz223@nenu.edu.cn

Table of Contents

1. Materials and Instrumentation
2. Synthesis of PZM from LZM
3. Crystal structure and characterizations of PZM
4. Photocatalytic reactions
5. Photocatalytic reaction mechanism
6. Determination of the Quantum Yield
7. General procedure
8. References

1. Materials and Instrumentation

Chemicals without additional descriptions were commercially available and used without further purification.

Single-crystal X-ray diffraction (SC-XRD) data was collected on Bruker Smart Apex II CCD diffractometer. Powder X-ray diffraction (PXRD) patterns were recorded on a Rigaku SmartLab X-Ray diffractometer operated at 40 kV/30 mA with Cu *K*α radiation (λ = 1.54178 Å) at room temperature. The PXRD patterns were collected at a scanning speed of 10 deg/min in the 2θ range of 3°–35°. UV-vis DRS spectrum of solid sample was recorded on a Cary 7000 spectrophotometer equipped with an integrating sphere. UV-vis spectrum of solution was collected on a SHIMADZU UV-2550 spectrophotometer. N_2 adsorption isotherm was performed at 77K using Micromeritics ASAP 2020. Mott-Schottky plots were conducted on electrochemical workstation CHI 660E (ChenHua Instrument, Shanghai). The morphologies of samples were characterized by a field emission scanning electron microscopy (SEM) with an acceleration voltage of 3.0 kV (HITACHI SU8000). Fourier transform infrared spectrum (FTIR) were recorded on a Mattson Alpha-Centauri spectrometer from 400 to 4000 cm^{-1} on KBr pellet. Thermogravimetry (TGA) measurement was performed under N_2 atmosphere using the Perkin-Elmer TGA-7 thermogravimetric analyzer from room temperature to 800 °C with a heating rate of 10 °C min^{-1}. Electron paramagnetic resonance (EPR) spectra were obtained on Bruker EPR spectrometer ER075 at room temperature. Gas chromatograph-mass spectrometry (GC-MS) was obtained using Agilent 6890/5973 with the following conditions: oven temperature, 300 °C; injector temperature, 290 °C; constant carrier gas flow rate, 1.0 mL/min; column temperature program, 10 °C/min, from 80 to 280 °C holding for 10 min. The MS ionization source was 70 eV and the temperature of the ion source was 200 °C. Edinburgh FLS920 fluorescence spectrometer was used to measure the lifetime and fluorescence quenching. X-ray photoelectron spectroscopy (XPS) spectra were collected at Kratos (ULTRA AXIS DLD) with monochrome Al *Kα* (*hv* = 1486.6 eV) radiation. And all binding energies were calibrated by referencing to C *1s* peak at 284.6 eV.

Photocatalytic experiments were conducted using a 300 W xenon lamp (420 nm < λ < 800 nm) under room temperature. The reaction was monitored by GC (Shimadzu Pro 2010) or thin layer chromatography (TLC) on silica gel 60 F_{254} plates. The purification of product was accomplished by silica gel chromatography. Solid-state ^{13}C NMR spectra were performed with a Bruker AVANCE NEO 400 MHz spectrometer. ^{1}H NMR and ^{19}F NMR spectra were recorded on AVANCE NEO 500 MHz spectrometers at 25 °C. Chemical shifts were reported in ppm from TMS within the solvent as the internal standard ($CDCl_3$ referenced at 7.27 ppm or DMSO-d_6 referenced at 2.50 ppm). Data for ^{1}H NMR were reported as follows: chemical shift (δ ppm), multiplicity (s = singlet, br. s = broad singlet, d = doublet, dd = doublet duplet, ddd = double triplet, t = triplet, q = quartet, m = multiplet) and coupling constants (Hz).

2. Synthesis of PZM from LZM

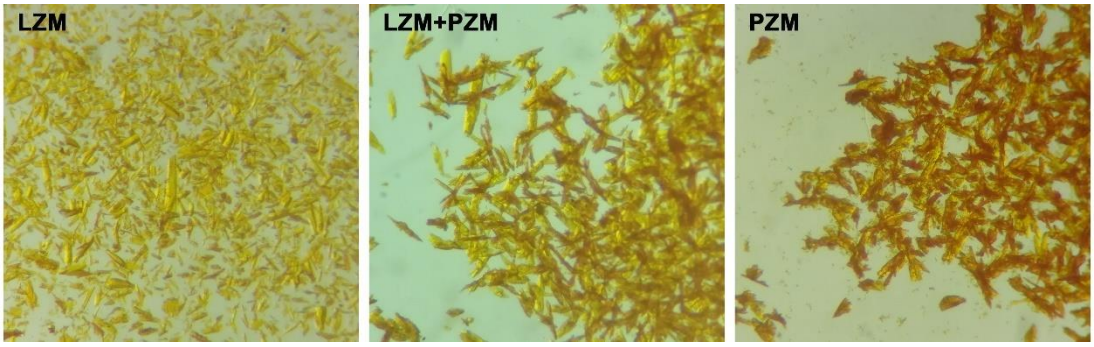

Figure S1. Optical micrograph images showing phase transition from LZM to PZM. The samples in the figures (from left to right) correspond to the addition of LZM (5 mg) and bpy (50 mg) in DMF/H_2O (4.5 mL) at 100 °C for 0, 3 and 5 days, respectively.

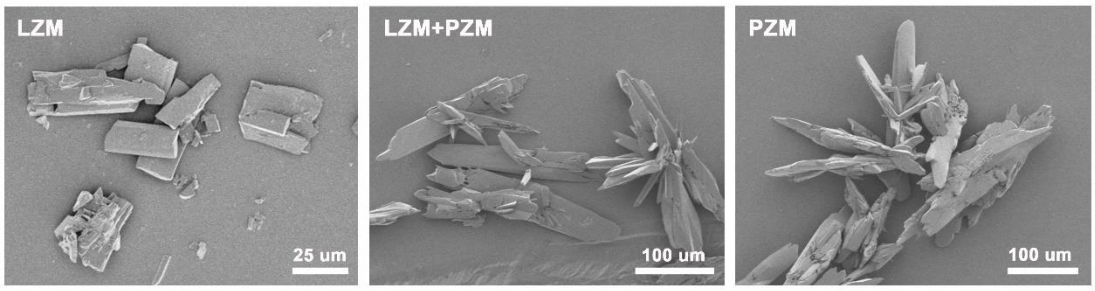

Figure S2. SEM images showing phase transition from LZM to PZM. The samples in the figures (from left to right) correspond to the addition of LZM (5 mg) and bpy (50 mg) in DMF/H_2O (4.5 mL) at 100 °C for 0, 3 and 5 days, respectively.

Table S1. Optimization on the synthetic conditions to prepare pure PZM.

Entry	bpy (mg)	DMF (mL)	H_2O (mL)	Time (day)	Product
1	20	4.5	0	3	LZM
2	20	4.0	0.5	3	LZM (major)+PZM
3	50	4.0	0.5	3	LZM+PZM (major)
4	80	4.0	0.5	3	LZM+PZM (major)
5	50	4.0	0.5	4	LZM+PZM (major)
6	50	4.0	0.5	5	PZM

Reaction conditions: LZM (5 mg), bpy and DMF/H_2O (4.5 mL), 100 °C.

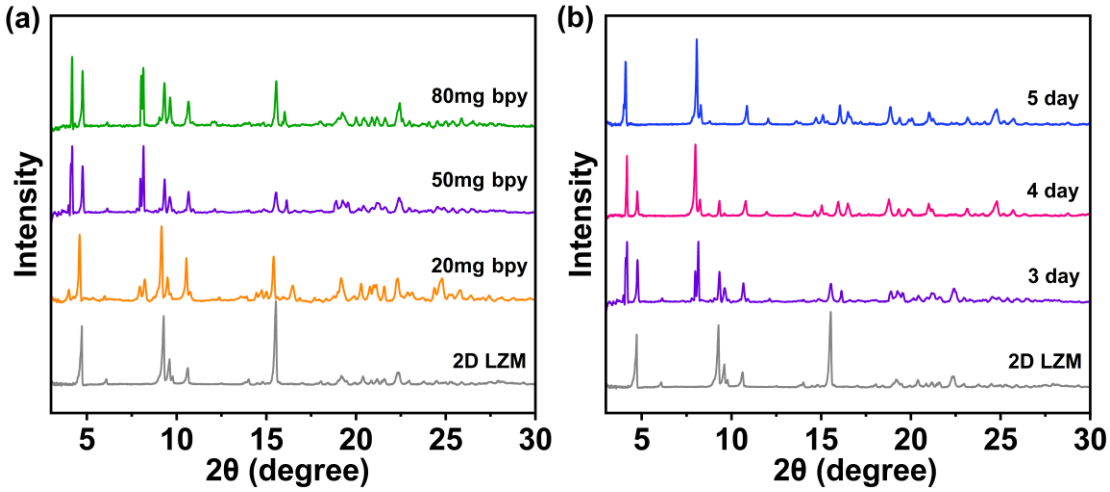

Figure S3. PXRD patterns of crystalline samples collected at different synthetic conditions. PXRD study showed that bpy dosage (a) and reaction time (b) play important role for the preparation of pure PZM (blue curve in figure b, and Figure S4). Reaction conditions for figure a: LZM (5 mg) and bpy in DMF/H_2O (4.5 mL), 100 °C, 3 days. Reaction conditions for figure b: LZM (5 mg) and bpy (50 mg) in DMF/H_2O (4.5 mL), 100 °C.

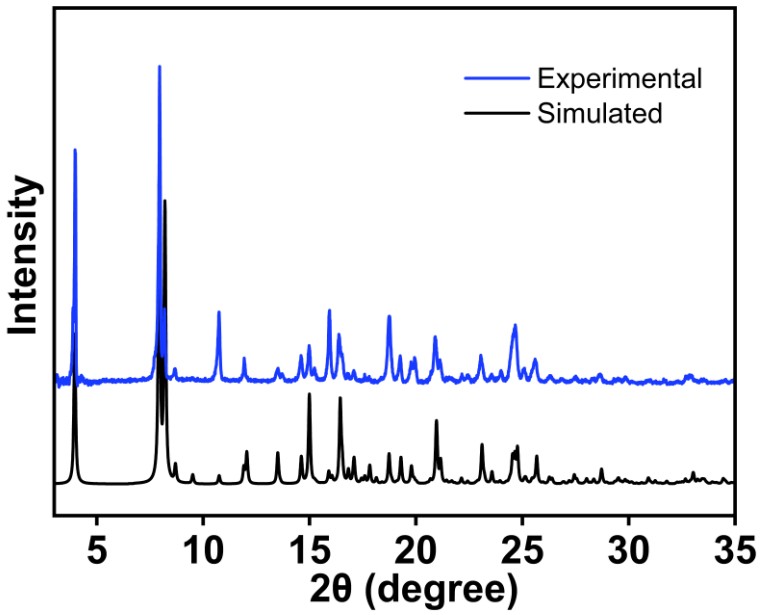

Figure S4. Experimental and simulated PXRD patterns of PZM.

3. Crystal structure and characterizations of PZM

Table S2. Crystal data and structural refinement of PZM and TEA/PZM.

Compound	PZM	TEA/PZM
empirical formula	$C_{37}H_{20}ZnNO_4$	$C_{43}H_{20}ZnN_2O_4$
formula weight	607.93	693.98
space group	$P2_1/c$	$P2_1/c$
crystal system	monoclinic	monoclinic
a / Å	23.7681(15)	23.7398(8)
b / Å	6.8546(4)	6.8646(2)
c / Å	21.6867(12)	21.7734(8)
α / °	90	90
β / °	110.437(2)	110.497(2)
γ / °	90	90
V / Å^3	3310.8(3)	3323.6(2)
Z	4	4
F (000)	1244	1416
θ range collected	3.109 to 26.810	1.987 to 63.883
limiting indices	$-30 \le h \le 30$ $-8 \le k \le 8$ $-27 \le l \le 27$	$-27 \le h \le 27$ $-7 \le k \le 6$ $-25 \le l \le 25$
Reflections collected/unique	28475 / 7088	17500 / 5430
data/restraints/parameters	7088 / 0 / 388	5431 / 100 / 506
R (int)	0.0580	0.0480
goodness-of-fit on F^2	1.083	1.037
Final R indices ([I>2σ(I)])	R_1 = 0.0317, wR_2 = 0.0803	R_1 = 0.0489, wR_2 = 0.1168
R indices (all data)	R_1 = 0.044, wR_2 = 0.0872	R_1 = 0.0732, wR_2 = 0.1287

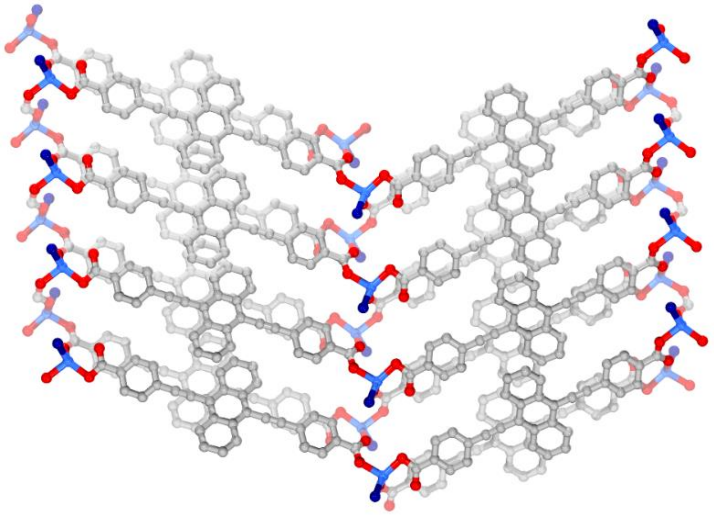

Figure S5. Layered building unit constructed by ADBEB and Zn^{2+} ions in PZM.

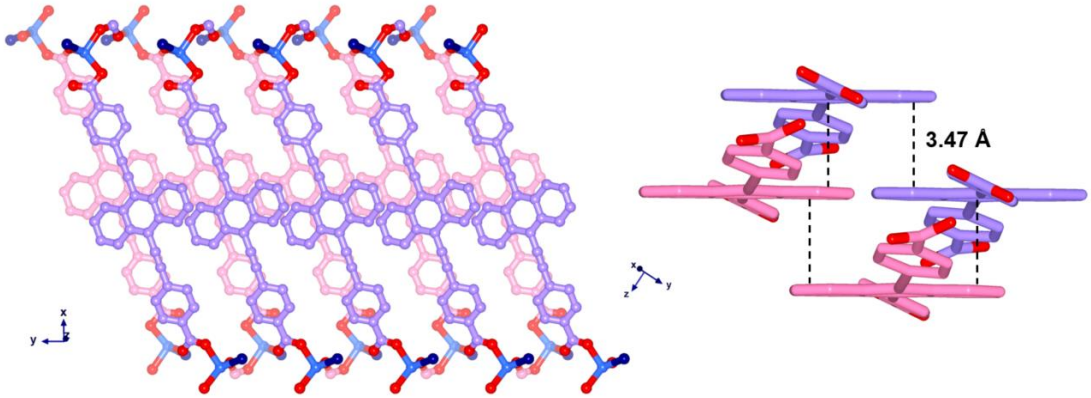

Figure S6. *π*-*π* interactions between ADBEB pillars in PZM (interplanar spacing of 3.47 Å).

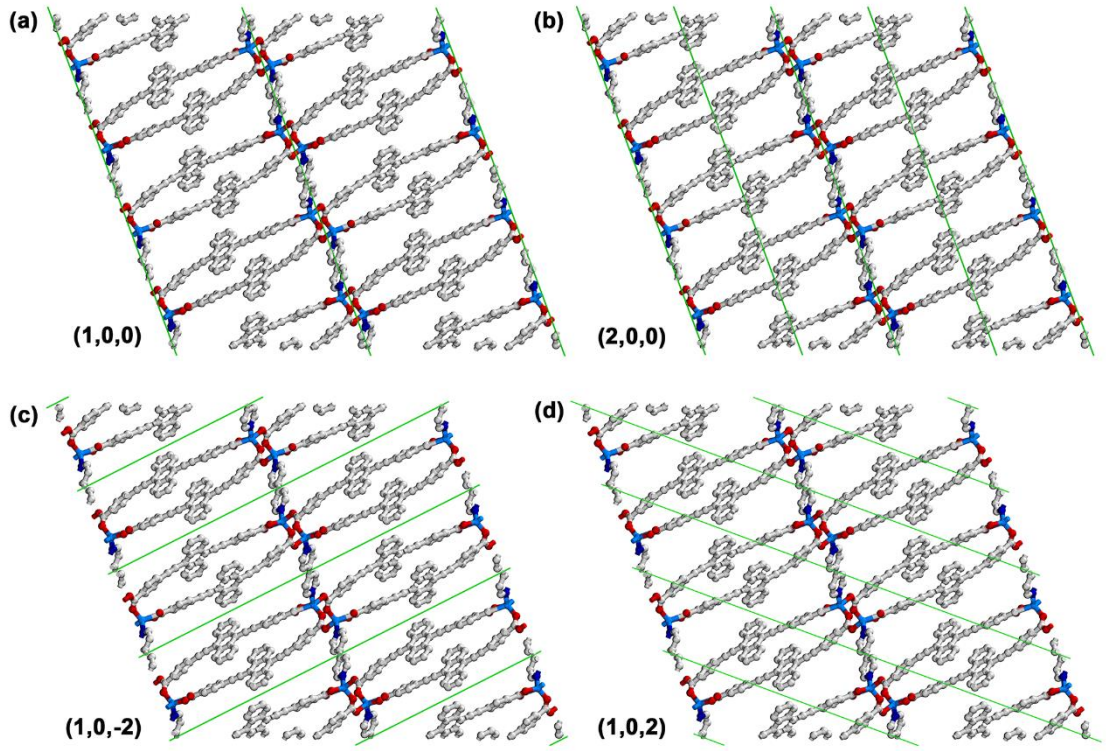

Figure S7. Crystal planes in PZM.

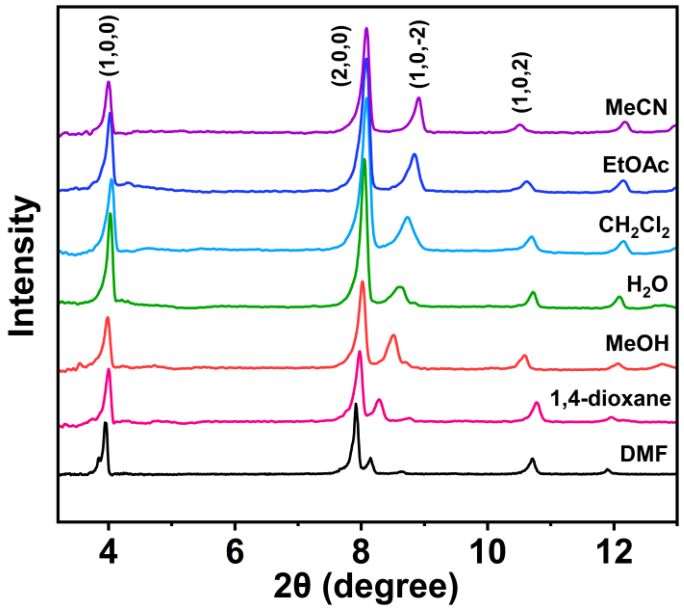

Figure S8. PXRD patterns of PZM after soaking in different solvents for one day at ambient conditions.

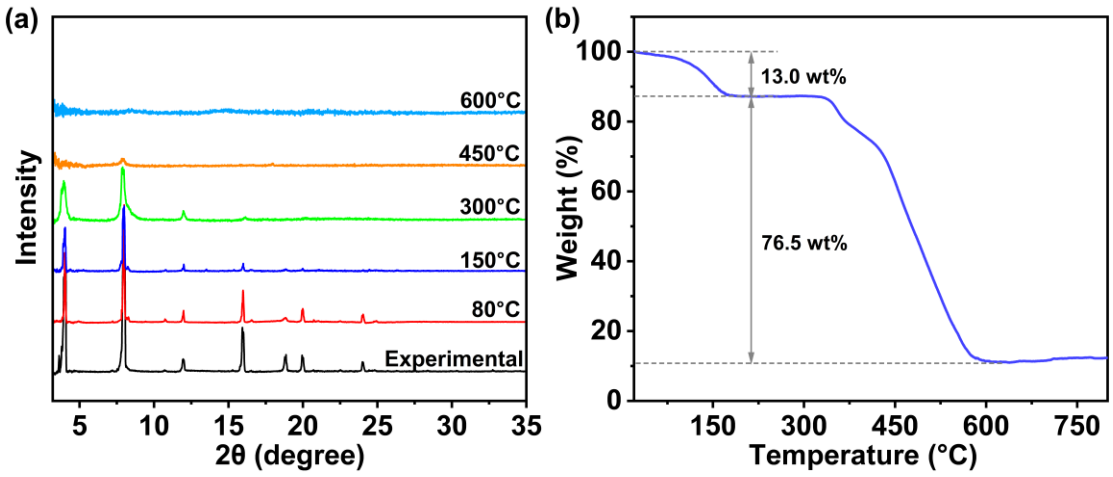

Figure S9. (a) PXRD patterns of PZM heated at different temperatures. (b) TG curve of PZM.

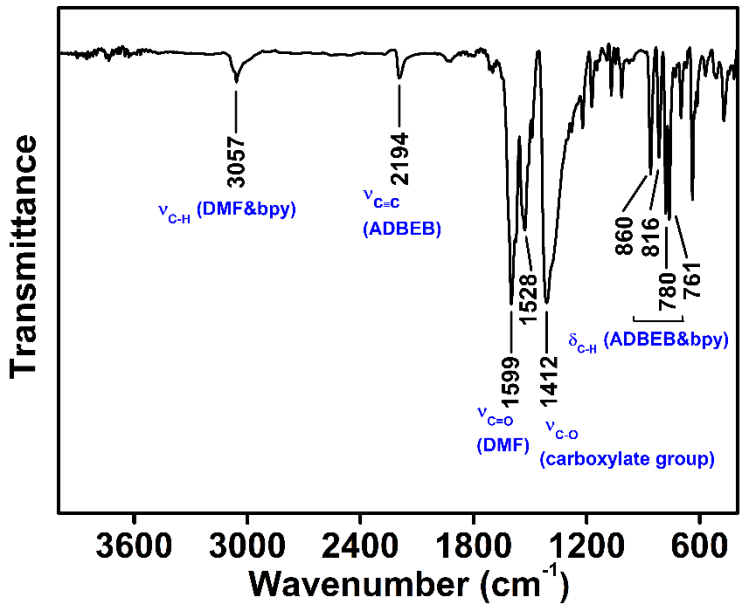

Figure S10. FTIR spectrum of PZM. The MOF shows a series of absorption peaks corresponding to ADBEB, bpy and DMF molecules in the structure. The characteristic absorption peak of ethynyl group ($\nu_{C\equiv C}$) in ADBEB is observed at 2194 cm^{-1} on FTIR spectrometry. The strong peak at 1412 cm^{-1} is attributed to the vibration of carboxylate groups in ADBEB. The out-of-plane vibration of C–H bonds in benzene groups of ADBEB and bpy locates at 860, 816, 780, and 761 cm^{-1}. Weak absorption peaks at 3057 cm^{-1} should be associated with the stretching vibration of C–H bonds in bpy and free guest of DMF. The peaks at 1599 and 1528 cm^{-1} correspond to carbonyl group in DMF.

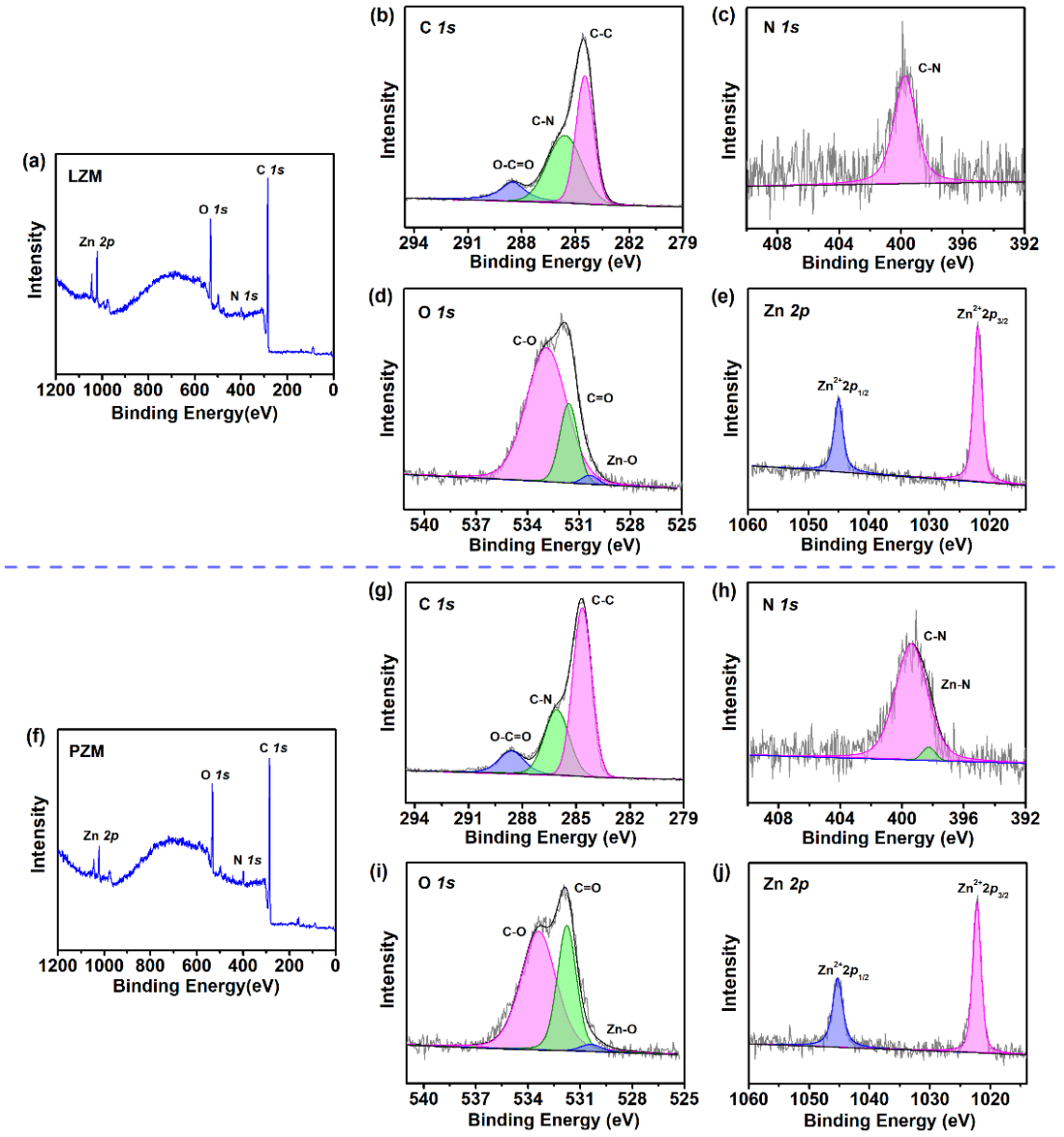

Figure S11. XPS of LZM (a-e) and PZM (f-j). It can be seen from the full spectra of LZM and PZM (Figures S11a and f) that several characteristic peaks appear at 284.6, 399.4, 531 and 1022 eV, which are attributed to C *1s*, N *1s*, O *1s* and Zn *2p*, respectively. The high-resolution spectrum of C *1s* (Figures S11b and g), showing three characteristic peaks at 284.6, 286 and 288 eV, respectively. Among them, the peak at 399.4 eV in the high-resolution spectrum of N *1s* of LZM (Figure S11c) is attributed to C–N. The N *1s* of PZM (Figure S11h) can be analyzed into two peaks of 398.3 and 399.4 eV, which belong to Zn–N and C–N respectively.[1] The high-resolution spectrum of O *1s* (Figures S11d and i) has three characteristic peaks at 530.4, 531.7 and 533 eV, which correspond to Zn–O coordination bond in Zn MOFs, C–O and C=O in ADBEB. The high-resolution spectrum of Zn *2p* (Figures S11e and j) are at 1022 and 1045 eV, which are attributed to the typical characteristic peaks of Zn^{2+}. The XPS analysis reveals that the coordination bonds of Zn–O and Zn–N appear in PZM, indicating that ADBEB and bpy performs coordination reaction with Zn^{2+}.

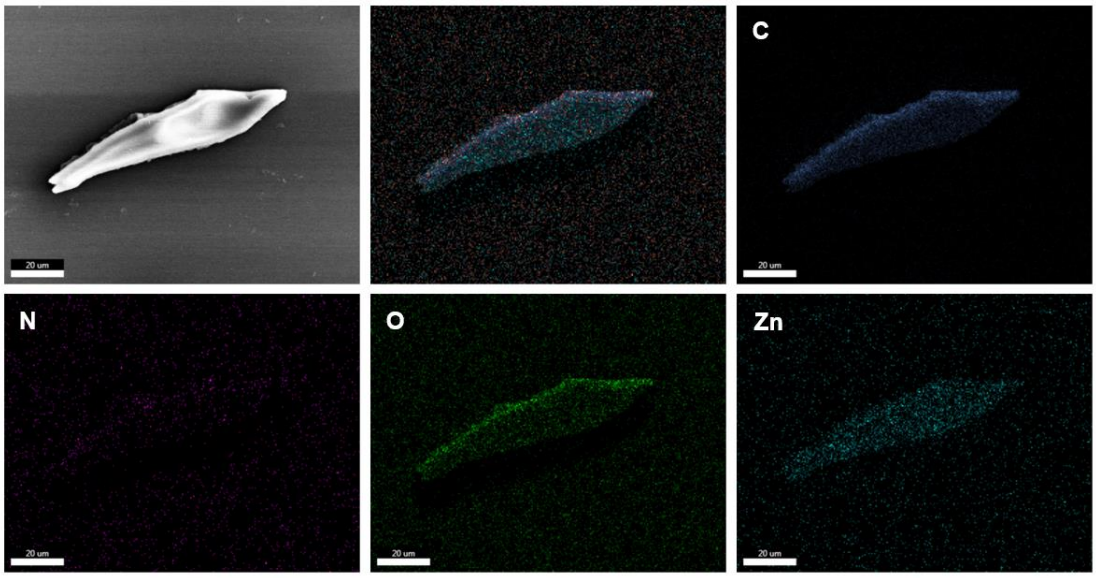

Figure S12. SEM element mapping of PZM.

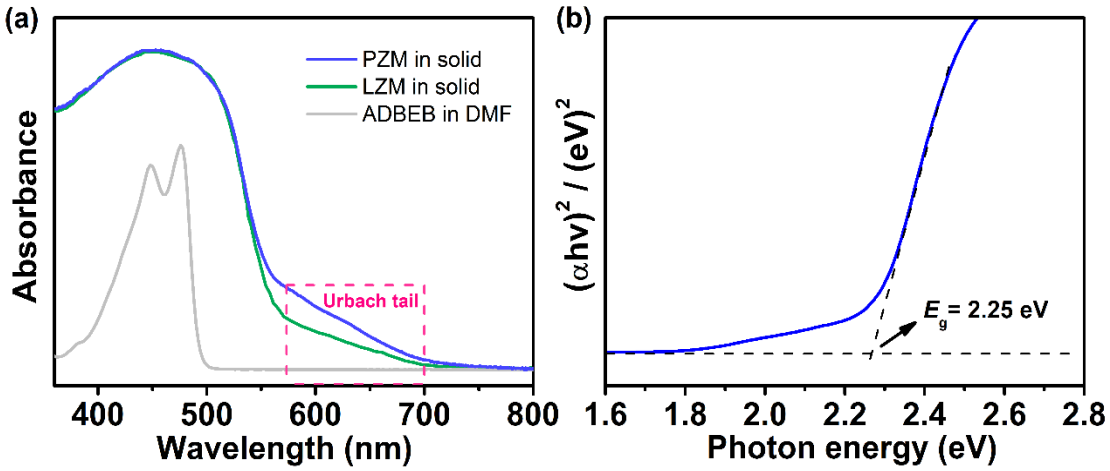

Figure S13. (a) UV-vis spectra of PZM and LZM in solid state, and ADBEB dissolved in DMF. (b) Tauc plot of PZM shows a bandgap energy of 2.25 eV.

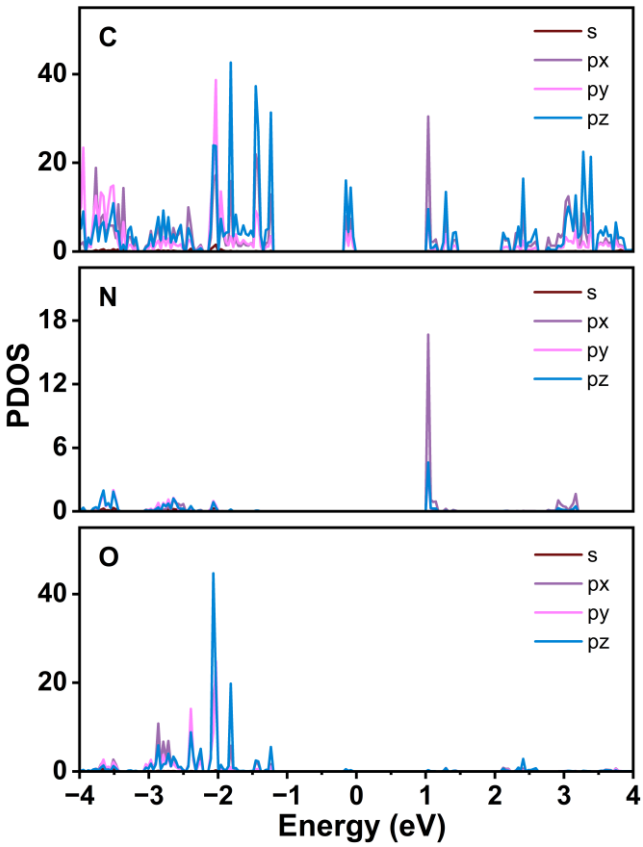

Figure S14. Partial density of states (PDOS) of C, N, and O in PZM.

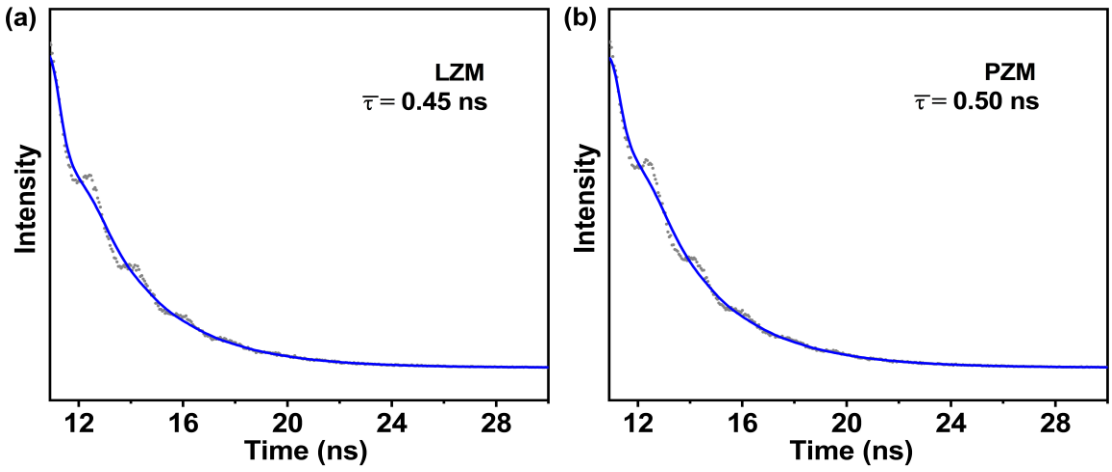

Figure S15. Fluorescence decay of (a) LZM and (b) PZM.

4. Photocatalytic reactions

Table S3. Photocatalytic perfluoroalkylation under different conditions.

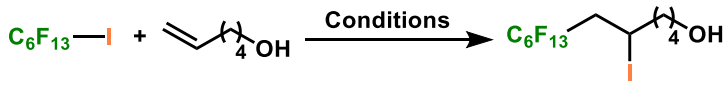

Entry	Photocatalyst	Amine	Irradiation	Yield (%)
1	PZM	TEA	*hv*	99
2	PZM	DIPEA	*hv*	53
3	PZM	EDA	*hv*	68
4	PZM	DIPA	*hv*	5
5	PZM	Me_2NBn	*hv*	41
6	PZM	-	*hv*	-
7	-	TEA	*hv*	trace
8	PZM	TEA	-	-

Reaction conditions: PZM (1.4 mg, 0.5 mol%), $C_6F_{13}I$ (0.4 mmol), 5-hexenol (0.2 mmol), amine (0.2 mmol), MeOH (400 μL), N_2, 30 min, visible light. Ethylenediamine (EDA), N,N-dimethylbenzylamine (Me_2NBn).

Table S4. Optimization on the solvent.

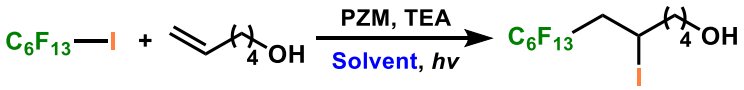

Entry	Solvent	Yield (%)
1	EtOAc	48
2	MeCN	64
3	H_2O	56
4	DMF	35
5	CH_2Cl_2	72
6	MeOH	99
7	1,4-Dioxane	29

Reaction conditions: PZM (1.4 mg, 0.5 mol%), $C_6F_{13}I$ (0.4 mmol), 5-hexenol (0.2 mmol), TEA (0.2 mmol), solvent (400 μL), N_2, 30 min, visible light.

Table S5. Optimization on dosages of PZM and TEA, and reaction time.

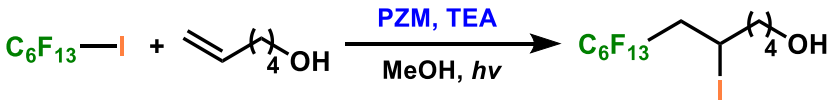

Entry	PZM (mg)	TEA (mmol)	Time (min)	Yield (%)
1	0.7	0.2	30	89
2	1.4	0.2	30	99
3	2.1	0.2	30	93
4	1.4	0.15	30	99
5	1.4	0.1	30	99
6	1.4	0.05	30	73
7	1.4	0.1	20	99
8	1.4	0.1	10	99
9	1.4	0.1	5	49

Reaction conditions: PZM, TEA, $C_6F_{13}I$ (0.4 mmol), 5-hexenol (0.2 mmol), MeOH (400 μL), N_2, visible light.

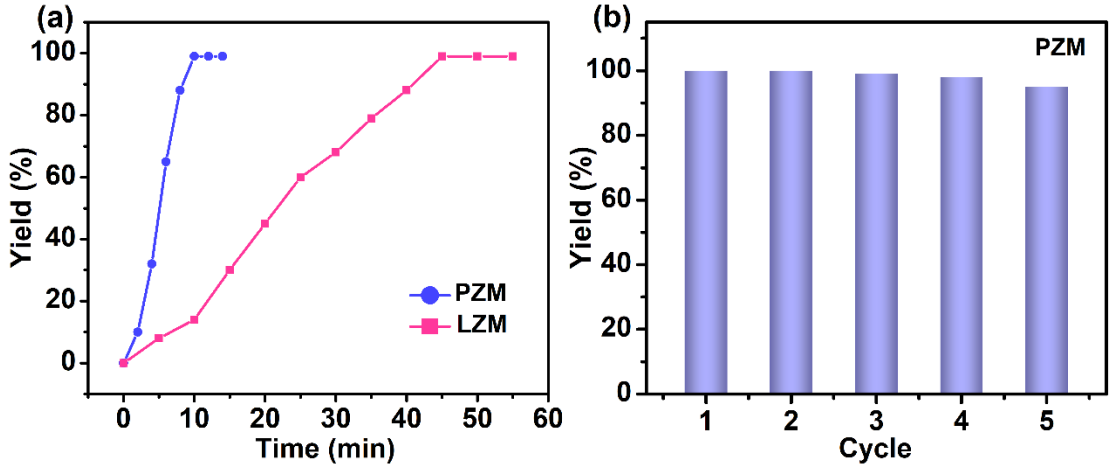

Figure S16. (a) Evolution of yields using PZM and LZM. (b) Cycling experiments using PZM.

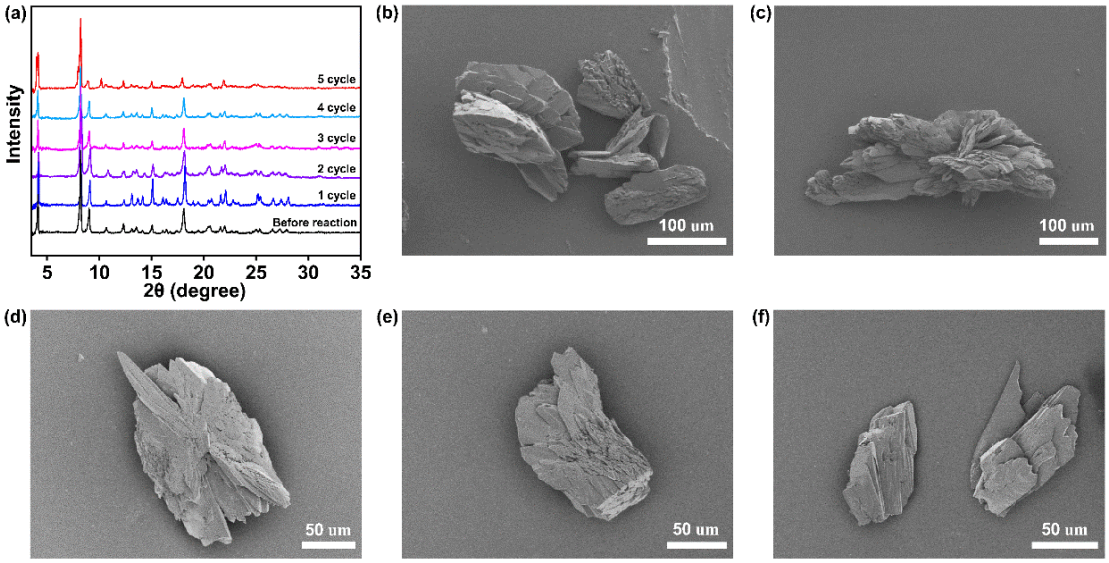

Figure S17. (a) PXRD patterns and (b-f) SEM images of PZM after photocatalytic reaction from the 1st-to-5th cycle.

Table S6. Comparison of the TOF values to prepare different perfluoro products using various photocatalysts.

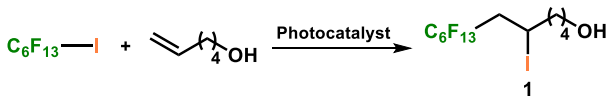

1

Photocatalyst	Time (h)	Yield (%)	TOF (h^{-1})	Refs
$[Ru(bpy)_3]Cl_2$	0.5	81	162	2
Eosin Y	1	54	54	3
PDI	4	98	490	4
Zn-MOF	4	89	44.5	5
am-CN	4	94	87	6
Iodo-Bodipy	20	35	1.8	7
diphenylacetaldehyde	16	80	0.5	8
NU-1000	12	89	3	9
Cd-MOF	24	99	1.4	10
Coumarin dye	36	45	0.5	11
p-anisaldehyde	23	94	0.2	12
NCNDs	24	80	4.8	13
LZM	0.75	99	132	This work
PZM	0.17	99	1187.8	This work

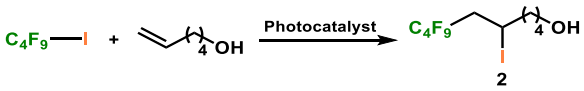

2

Photocatalyst	Time (h)	Yield (%)	TOF (h^{-1})	Refs
PDI	4	95	475	4
Cd-MOF	24	99	1.4	10
NU-1000	12	85	2.8	9
NCNDs	24	81	4.8	13
LZM	0.83	99	119.3	This work
PZM	0.17	99	1187.8	This work

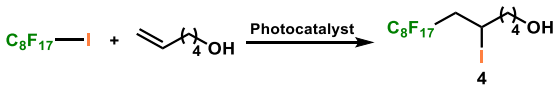

4

Photocatalyst	Time (h)	Yield (%)	TOF (h^{-1})	Refs
$[Ru(bpy)_3]Cl_2$	0.5	81	162	2
PDI	4	96	480	4
NU-1000	12	93	3.1	9
NCNDs	24	83	4.9	13
LZM	0.75	99	132	This work
PZM	0.17	99	1187.8	This work

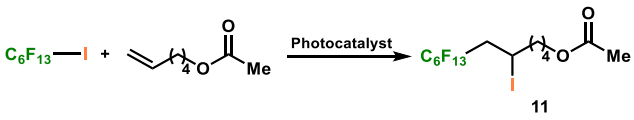

11

Photocatalyst	Time (h)	Yield (%)	TOF (h^{-1})	Refs
PDI	4	97	485	4
Zn-MOF	4	96	45.5	5
am-CN	4	72	84	6
NCNDs	24	83	5	13
LZM	1.5	99	66	This work
PZM	0.17	99	1187.8	This work

TOF = product (μmol)/[active site amount (μmol) × reaction time (h)].

5. Photocatalytic reaction mechanism

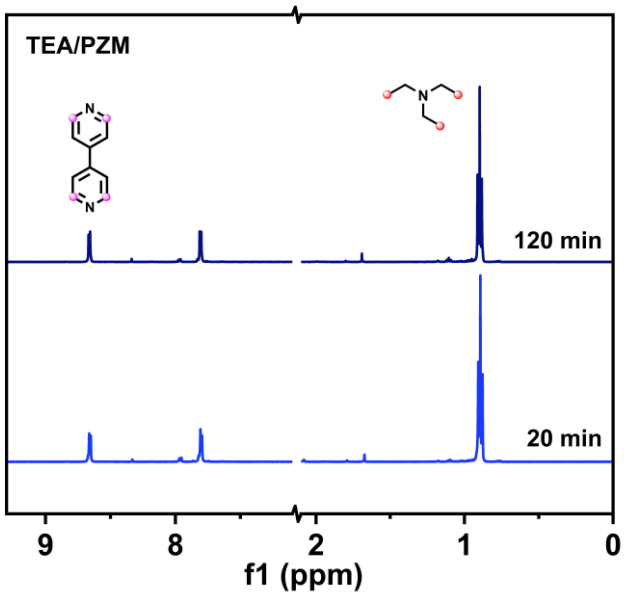

Figure S18. ^{1}H NMR spectra of TEA/PZM after 3D PZM soaking TEA for 20 min and 120 min. Hydrogen on bpy ligand in PZM (8.63 ppm) was used as a reference to quantitative analysis of the adsorbed TEA (0.89 ppm, -CH_3). The amounts of TEA adsorbed by PZM was calculated to be 2.10 (20 min) and 2.13 (120 min) molecules per unit cell of the MOF, respectively. These values suggest the maximum adsorption capacity can be reached at 20 min (see also Fig. 4b in the paper).

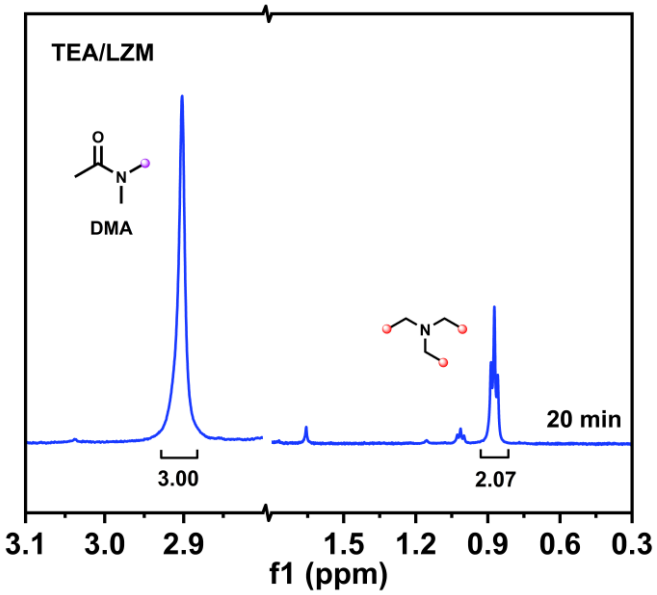

Figure S19. ^{1}H NMR spectrum of TEA/LZM after soaking 2D LZM in TEA for 20 min. Hydrogen on the DMA molecule (2.90 ppm, -CH_3) coordinated in LZM was used as a reference to quantitative analysis of the adsorbed TEA (0.89 ppm, -CH_3). The TEA adsorption capacity of LZM was calculated to be 0.23 molecules per unit cell of the MOF, which is much smaller than that shown by PZM.

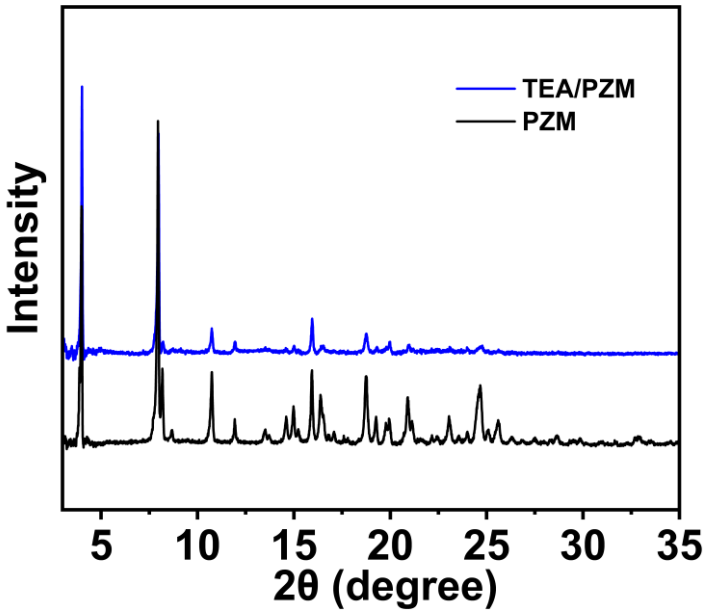

Figure S20. PXRD patterns of PZM and TEA/PZM.

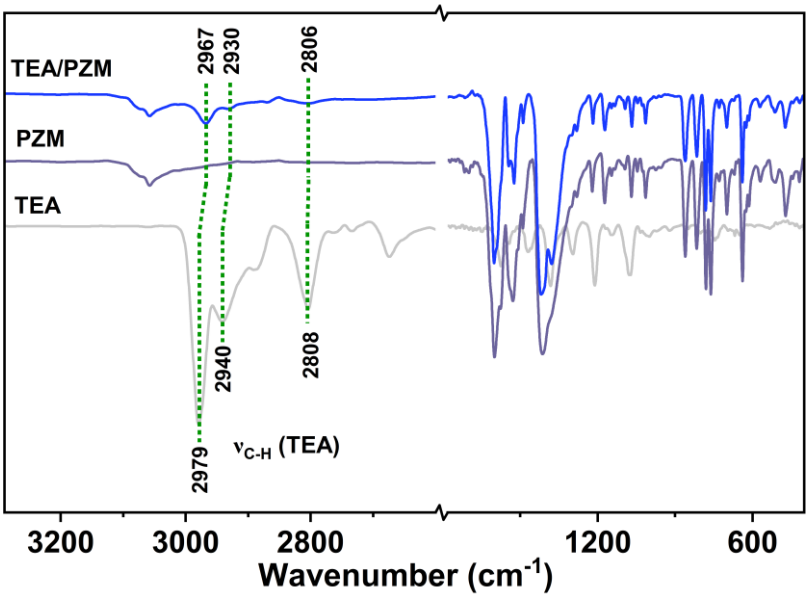

Figure S21. FTIR spectra of TEA/PZM, PZM and TEA. As shown in the figure, TEA/PZM exhibits emerging peaks at 2967, 2930 and 2806 cm^{-1} attributed to C-H vibration of loaded TEA molecules. It is notable that these peaks shifted significantly towards lower wavenumbers as compared with the free TEA molecules, displaying the host-guest interaction between PZM and TEA.

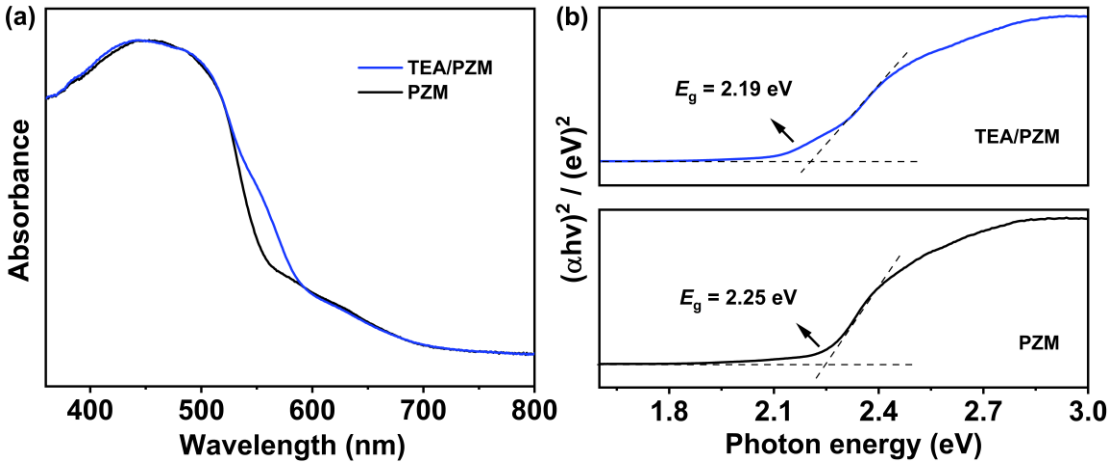

Figure S22. (a) UV-vis spectra and (b) Tauc plots of PZM and TEA/PZM.

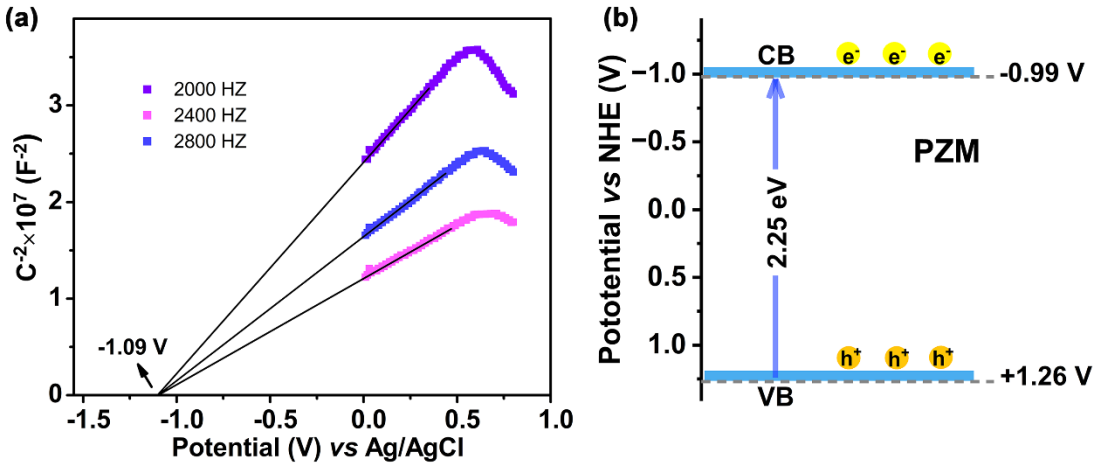

Figure S23. (a) Mott-Schottky plots of PZM at different frequencies. (b) CB, VB and bandgap of PZM. The flat-band potential evidenced by the intersection of the plots locates at −1.09 V *vs*. Ag/AgCl. In view that the measured flat-band potentials would be typically 0.10 V below the bottom of the conduction bands,[14] the CB position of PZM should be −1.19 V (*vs*. Ag/AgCl). The CB and VB potentials were then converted by a relationship of $E_{NHE} = E_{Ag/AgCl} + 0.197$.[15] Thus, the CB and VB locate at −0.99 and 1.26 V (*vs.* NHE), respectively.

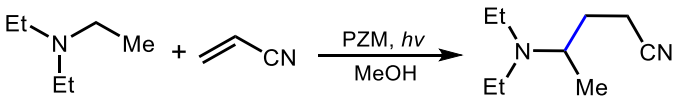

Chemical Formula: $C_9H_{18}N_2$
Exact Mass: 154.15
Molecular Weight: 154.26
m/z: 154.15 (100.0%), 155.15 (9.7%)
Elemental Analysis: C, 70.08; H, 11.76; N, 18.16

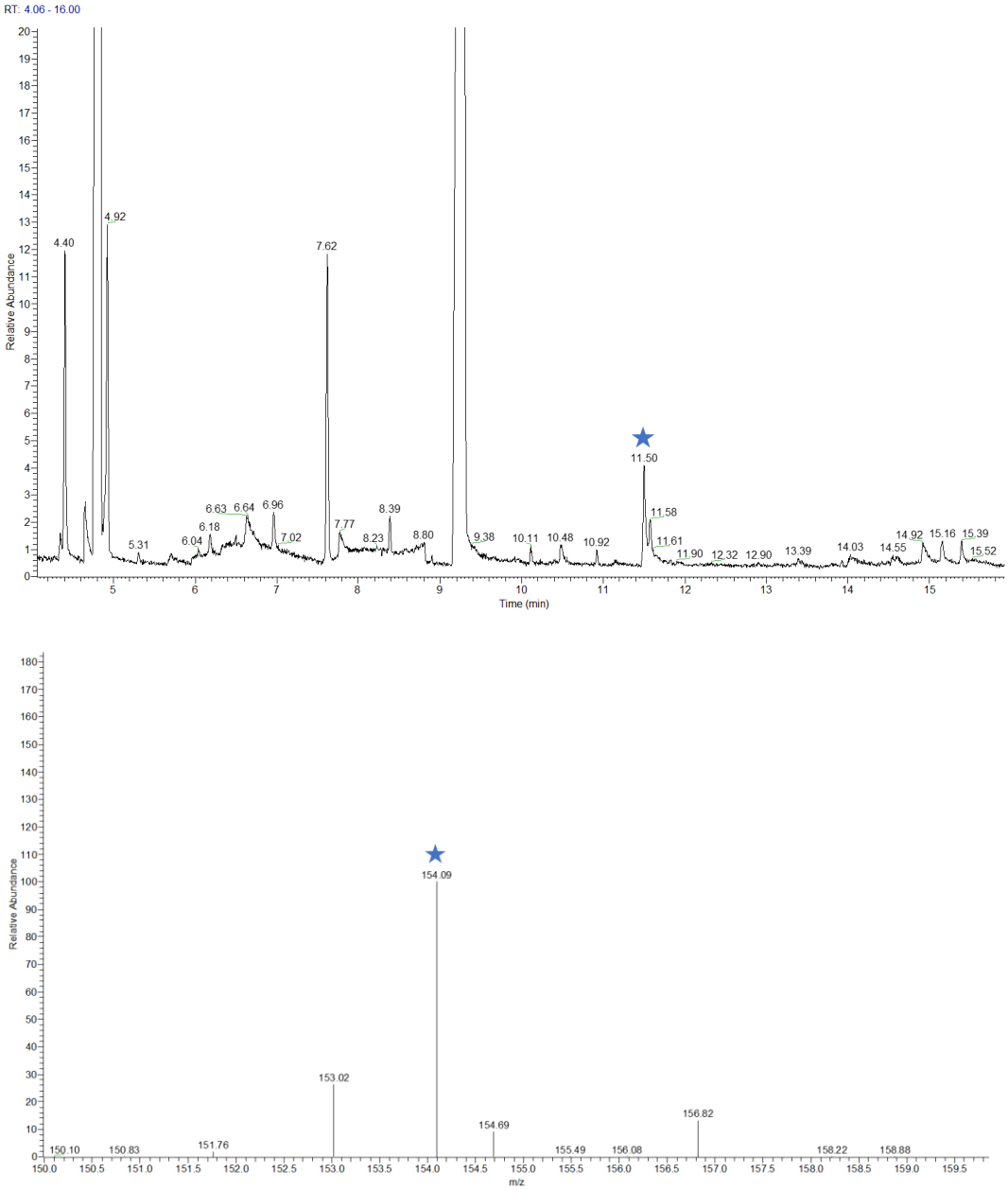

Figure S24. GC-MS spectrum for the detection of α-aminoalkyl radical. Peaks labeled by asterisk in the figures are related to the radical-adduct of TEA with acrylonitrile.

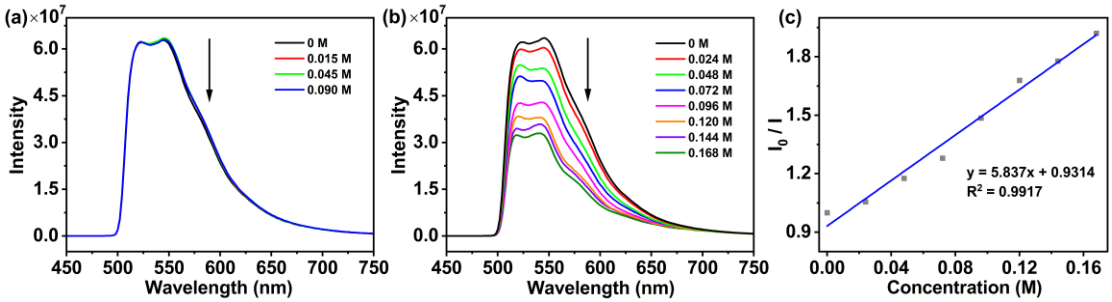

Figure S25. Fluorescence quenching of PZM by (a) $C_6F_{13}I$ and (b) TEA. (c) Stern-Volmer plot of the quenching using TEA.

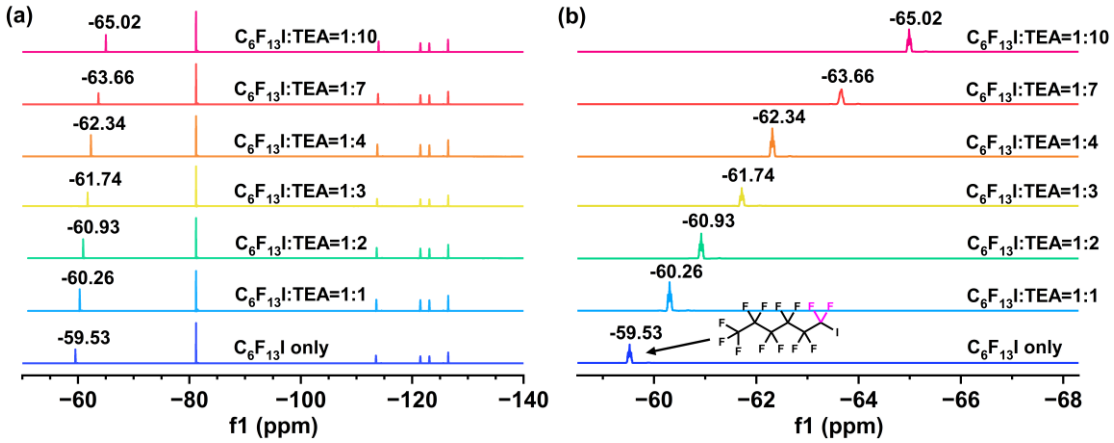

Figure S26. ^{19}F NMR shift of $C_6F_{13}I$ with TEA: (a) original spectrogram and (b) locally enlarged spectrogram.

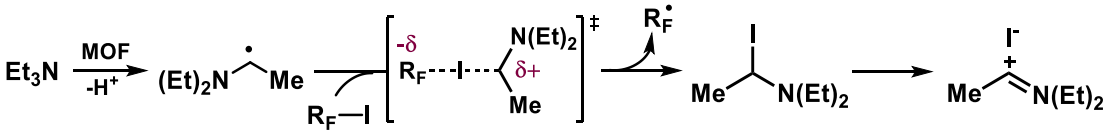

Figure S27. Process diagram of TEA in the photocatalytic reaction.

6. Determination of the Quantum Yield

6.1 Determination of the photon flux at 460 nm:

The photon flux of the spectrophotometer was determined following the work of Yoon and coworkers,[16] utilizing standard ferrioxalate actinometry.[17,18] A 0.15 M solution of potassium ferrioxalate was prepared by dissolving 2.21 g of potassium ferrioxalate hydrate in 30 mL of 0.05 M H_2SO_4. A buffered solution of phenanthroline was prepared by dissolving 50 mg of phenanthroline and 11.25 g of sodium acetate in 50 mL of 0.5 M H_2SO_4. Both solutions were stored in the dark. To determine the photon flux of the spectrophotometer, 2.0 mL of the potassium ferrioxalate solution was placed in the vial and irradiated for 90.0 s at 460 nm. After irradiation, 0.35 mL of the phenanthroline solution was added to the vial. The solution was allowed to rest for 1 h (complete coordination of ferrous ions to phenanthroline). The absorbances of irradiated and non-irradiated solutions at 510 nm were measured respectively. Conversion was calculated using eq 1:

$$Mol\ Fe^{2+} = \frac{V \times \Delta A}{l \times \varepsilon} \tag{1}$$

In this equation, V is the total volume of the solution after addition of the phenanthroline (0.00235 L), ΔA is the difference in the absorbance at 510 nm between the irradiated and the non-irradiated solutions, l is the path length (1.0 cm), and ε is the molar absorptivity at 510 nm (11100 L mol^{-1} cm^{-1}).[16-18] The mole of Fe^{2+} was calculated to be 4.078×10^{-7}.

The photon flux can be calculated using eq 2:

$$photon\ flux = \frac{Mol\ Fe^{2+}}{\Phi \times t \times f} \tag{2}$$

In this equation, Φ is the quantum yield of the ferrioxalate actinometer (Φ = 0.92 for a 0.15 M solution at 460 nm),[19,20] t is the time of the irradiation (90.0 s), and f is the fraction of the light absorbed at 460 nm, which can be calculated using eq 3 based on the measured absorbance (A) (see Figure S28).

$$f = 1 - 10^{-A} \tag{3}$$

Thus, the f value was determined to be 0.995 and the photon flux of the spectrophotometer was calculated (average of three experiments) to be 4.95×10^{-9} einstein s^{-1}.

6.2 Determination of the quantum yield:

A 4 mL vial was charged with PZM (1.4 mg), $C_6F_{13}I$ (0.4 mmol), 5-hexenol (0.2 mmol), TEA (0.1 mmol), MeOH (400 μL). The sample was stirred and irradiated at 460 nm for 60 s (1 min). The yield of the product was 5% by GC utilizing an internal standard, and the quantum yield was determined to be 33839 using the following equation:

$$\Phi = \frac{mol\ product}{flux \times t \times f} \quad (4)$$

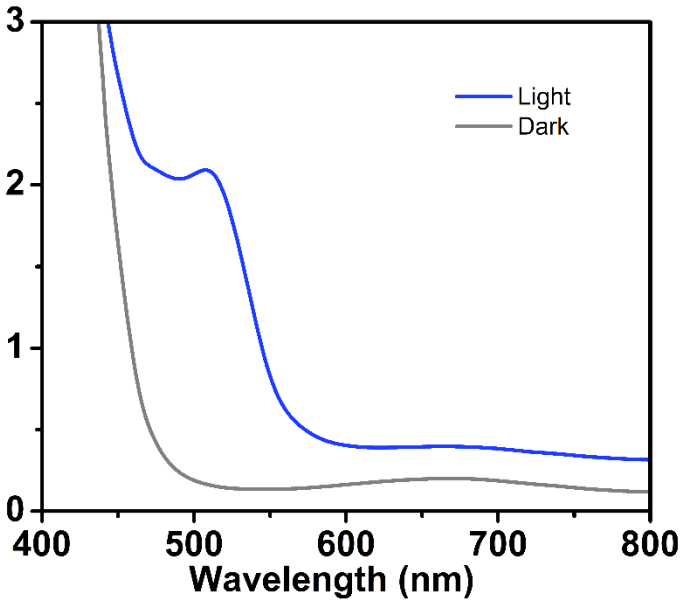

Figure S28. Absorbance of the ferrioxalate actinometer solution.

7. General procedure

7,7,8,8,9,9,10,10,11,11,12,12,12-Tridecafluoro-5-iodododecan-1-ol (1)

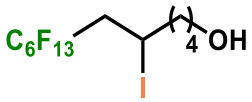

The general procedure was followed using PZM (1.4 mg, 0.5 mol%), $C_6F_{13}I$ (86 µL, 0.4 mmol), 5-hexenol (24 µL, 0.2 mmol), TEA (14 µL, 0.1 mmol), MeOH (400 µL), 10 min. Purification by flash column chromatography (gradient eluent from hexane to 20:1 hexane:AcOEt) afforded the title compound (99% yield).
^{1}H NMR (500 MHz, $CHCl_3$): δ 4.37 – 4.31 (m, 1H), 3.60 (t, *J* = 5.9 Hz, 2H), 2.89 – 2.68 (m, 2H), 1.82 – 1.70 (m, 2H), 1.60 – 1.40 (m, 4H).[10]

7,7,8,8,9,9,10,10,10-nonafluoro-5-iodododecan-1-ol (2)

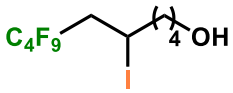

The general procedure was followed using PZM (1.4 mg, 0.5 mol%), C_4F_9I (69 µL, 0.4 mmol), 5-hexenol (24 µL, 0.2 mmol), TEA (14 µL, 0.1 mmol), MeOH (400 µL), 10 min. Purification by flash column chromatography (gradient eluent from hexane to 20:1 hexane:AcOEt) afforded the title compound (99% yield).
^{1}H NMR (500 MHz, $CHCl_3$): δ 4.34 – 4.29 (m, 1H), 3.61 (t, *J* = 5.6 Hz, 2H), 2.94 – 2.70 (m, 2H), 1.88 – 1.78 (m, 2H), 1.63 – 1.44 (m, 4H).[10]

Tert-butyl (4,4,5,5,6,6,7,7,7-nonafluoro-2-iodoheptyl)carbamate (3)

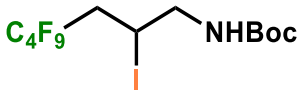

The general procedure was followed using PZM (1.4 mg, 0.5 mol%), C_4F_9I (69 µL, 0.4 mmol), *tert*-butyl-*N*-allylcarbamate (33.6 mg, 0.2 mmol), TEA (14 µL, 0.1 mmol), MeOH (400 µL), 1 h. Purification by flash column chromatography (gradient eluent from hexane to 20:1 hexane:AcOEt) afforded the title compound (85% yield).
^{1}H NMR (500 MHz, $CHCl_3$): δ 4.95 (br s, 1H), 4.36 (p, *J* = 6.6 Hz, 1H), 3.62 – 3.37 (m, 2H), 2.89 – 2.64 (m, 2H), 1.42 (s, 9H).[21]

7,7,8,8,9,9,10,10,11,11,12,12,13,13,14,14,14-heptadecafluoro-5-iodotetradecan-1-ol (4)

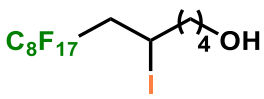

The general procedure was followed using PZM (1.4 mg, 0.5 mol%), $C_8F_{17}I$ (105 µL, 0.4 mmol), 5-hexenol (24 µL, 0.2 mmol), TEA (14 µL, 0.1 mmol), MeOH (400 µL), 10 min. Purification by flash column chromatography (gradient eluent from hexane to 20:1 hexane:AcOEt) afforded the title compound (99% yield).
^{1}H NMR (500 MHz, $CHCl_3$): δ 4.37 – 4.28 (m, 1H), 3.68 (t, *J* = 7.5 Hz, 2H), 3.00 – 2.67 (m, 2H), 1.92 – 1.76 (m, 2H), 1.70 – 1.41 (m, 4H), 1.40 – 1.22 (br s, 1H).[2]

tert-butyl(4,4,5,5,6,6,7,7,8,8,9,9,10,10,11,11,11-heptadecafluoro-2-iodoundecyl)carbamate (5)

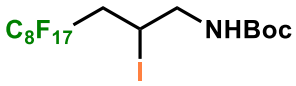

The general procedure was followed using PZM (1.4 mg, 0.5 mol%), $C_8F_{17}I$ (105 µL, 0.4 mmol), *tert*-butyl-*N*-allylcarbamate (33.6 mg, 0.2 mmol), TEA (14 µL, 0.1 mmol), MeOH (400 µL), 1 h. Purification by flash column chromatography (gradient eluent from hexane to 20:1 hexane:AcOEt) afforded the title compound (98% yield).
^{1}H NMR (500 MHz, $CHCl_3$): δ 5.05 – 4.83 (br s, 1H), 4.40 – 4.31 (m, 1H), 3.65 – 3.33 (m, 2H), 2.91 – 2.68 (m, 2H), 1.45 (s, 9H).[2]

5-(Perfluorooctyl)-4-iodopentyl acetate (6)

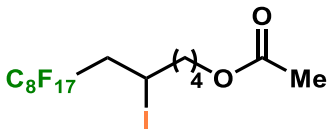

The general procedure was followed using PZM (1.4 mg, 0.5 mol%), $C_8F_{17}I$ (105 µL, 0.4 mmol), 4-pentenyl acetate (32 µL, 0.2 mmol), TEA (14 µL, 0.1 mmol), MeOH (400 µL), 10 min. Purification by flash column chromatography (gradient eluent from hexane to 20:1 hexane:AcOEt) afforded the title compound (99% yield).
^{1}H NMR (500 MHz, $CHCl_3$): δ 4.38 – 4.35 (m, 1H), 4.15 – 4.10 (m, 2H), 3.01 – 2.73 (m, 2H), 2.05 (s, 3H), 1.90 – 1.72 (m, 4H).[22]

1-bromo-5-iodo-6-perfluorooctylhexane (7)

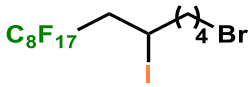

The general procedure was followed using PZM (1.4 mg, 0.5 mol%), $C_8F_{17}I$ (105 µL, 0.4 mmol), 6-bromo-1-hexene (27 µL, 0.2 mmol), TEA (14 µL, 0.1 mmol), MeOH (400 µL), 1 h. Purification by flash column chromatography (gradient eluent from hexane to 20:1 hexane:AcOEt) afforded the title compound (95% yield).
^{1}H NMR (500 MHz, $CHCl_3$): δ 4.38 – 4.32 (m, 1H), 3.41 (t, *J* = 7.0 Hz, 2H), 3.01 – 2.84 (m, 1H), 2.83 – 2.66 (m, 1H), 1.99 – 1.63 (m, 5H), 1.60 – 1.50 (m, 1H).[4]

1,1,1,2,2,3,3,4,4,5,5,6,6-tridecafluoro-8-iodododecane (8)

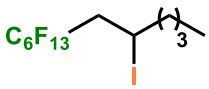

The general procedure was followed using PZM (1.4 mg, 0.5 mol%), $C_6F_{13}I$ (86 µL, 0.4 mmol), 1-hexene (25 µL, 0.2 mmol), TEA (14 µL, 0.1 mmol), MeOH (400 µL), 1 h. Purification by flash column chromatography (gradient eluent from hexane to 20:1 hexane:AcOEt) afforded the title compound (83% yield).
^{1}H NMR (500 MHz, $CHCl_3$): δ 4.41 – 4.24 (m, 1H), 3.02 – 2.65 (m, 2H), 1.92 – 1.70 (m, 2H), 1.57 – 1.20 (m, 4H), 0.92 (t, *J* = 7.2 Hz, 3H).[23]

1,1,1,2,2,3,3,4,4,5,5,6,6-Tridecafluoro-8-iodotetradecane (9)

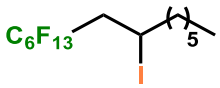

The general procedure was followed using PZM (1.4 mg, 0.5 mol%), $C_6F_{13}I$ (86 µL, 0.4 mmol), 1-octene (32 µL, 0.2 mmol), TEA (14 µL, 0.1 mmol), MeOH (400 µL), 1 h. Purification by flash column chromatography (gradient eluent from hexane to 20:1 hexane:AcOEt) afforded the title compound (87% yield).
^{1}H NMR (500 MHz, $CHCl_3$): δ 4.35 – 4.28 (m, 1H), 2.99 – 2.70 (m, 2H), 1.87 – 1.71 (m, 2H), 1.58 – 1.47 (m, 1H), 1.45 – 1.23 (m, 7H), 0.90 (t, *J* = 6.6 Hz, 3H).[24]

1,1,1,2,2,3,3,4,4,5,5,6,6-tridecafluoro-8-iodohexadecane (10)

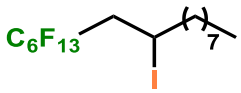

The general procedure was followed using PZM (1.4 mg, 0.5 mol%), $C_6F_{13}I$ (86 µL, 0.4 mmol), 1-decen (38 µL, 0.2 mmol), TEA (14 µL, 0.1 mmol), MeOH (400 µL), 1 h. Purification by flash column chromatography (gradient eluent from hexane to 20:1 hexane:AcOEt) afforded the title compound (99% yield).
^{1}H NMR (500 MHz, $CHCl_3$): δ 4.31 (tt, *J* = 8.8, 4.4 Hz, 1H), 3.00 – 2.68 (m, 2H), 1.87 – 1.70 (m, 2H), 1.57 – 1.28 (m, 12H), 0.88 (t, *J* = 6.4 Hz, 3H).[8]

7,7,8,8,9,9,10,10,11,11,12,12,12-tridecafluoro-5-iodododecyl acetate (11)

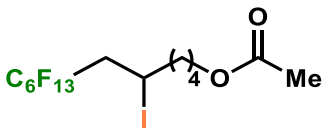

The general procedure was followed using PZM (1.4 mg, 0.5 mol%), $C_6F_{13}I$ (86 µL, 0.4 mmol), 5-hexenyl acetate (32 µL, 0.2 mmol), TEA (14 µL, 0.1 mmol), MeOH (400 µL), 10 min. Purification by flash column chromatography (gradient eluent from hexane to 20:1 hexane:AcOEt) afforded the title compound (99% yield).
^{1}H NMR (500 MHz, $CHCl_3$): δ 4.33 (ddd, *J* = 13.3, 8.4, 5.1 Hz, 1H), 4.05 (t, *J* = 6.3 Hz, 2H), 3.00 – 2.65 (m, 2H), 1.99 (s, 3H), 1.88 – 1.40 (m, 6H).[4]

5-Perfluoroalkyl-4-iodopentan-1-ol (12)

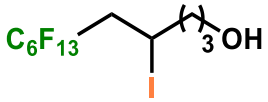

The general procedure was followed using PZM (1.4 mg, 0.5 mol%), $C_6F_{13}I$ (86 µL, 0.4 mmol), 4-penten-1-ol (20 µL, 0.2 mmol), TEA (14 µL, 0.1 mmol), MeOH (400 µL), 10 min. Purification by flash column chromatography (gradient eluent from hexane to 20:1 hexane:AcOEt) afforded the title compound (92% yield).
^{1}H NMR (500 MHz, $CHCl_3$): δ 4.37 – 4.30 (m, 1H), 3.65 (t, *J* = 9.9 HZ, 2H), 2.10 – 1.98 (m, 2H), 1.80 – 1.75 (m, 2H), 1.70 – 1.63 (m, 2H).[25]

***Tert*-butyl (4,4,5,5,6,6,7,7,8,8,9,9,9-tridecafluoro-2-iodononyl)carbamate (13)**

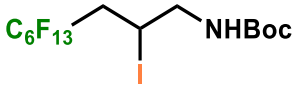

The general procedure was followed using PZM (1.4 mg, 0.5 mol%), $C_6F_{13}I$ (86 µL, 0.4 mmol), *tert*-butyl-*N*-allylcarbamate (33.6 mg, 0.2 mmol), TEA (14 µL, 0.1 mmol), MeOH (400 µL), 10 min. Purification by flash column chromatography (gradient eluent from hexane to 20:1 hexane:AcOEt) afforded the title compound (80% yield).
^{1}H NMR (500 MHz, $CHCl_3$): δ 4.99 (br s, 1H), 4.40 – 4.32 (m, 1H), 3.61 – 3.40 (m, 2H), 2.95 – 2.68 (m, 2H), 1.44 (s, 9H).[24]

12-bromo-1,1,1,2,2,3,3,4,4,5,5,6,6-tridecafluoro-8-iodododecane (14)

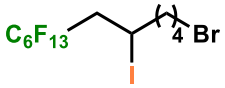

The general procedure was followed using PZM (1.4 mg, 0.5 mol%), $C_6F_{13}I$ (86 µL, 0.4 mmol), 6-bromo-1-hexene (27 µL, 0.2 mmol), TEA (14 µL, 0.1 mmol), MeOH (400 µL), 1 h. Purification by flash column chromatography (gradient eluent from hexane to 20:1 hexane:AcOEt) afforded the title compound (92% yield).
^{1}H NMR (500 MHz, $CHCl_3$): δ 4.37 – 4.29 (m, 1H), 3.40 (t, *J* = 7.0 Hz, 2H), 3.01 – 2.85 (m, 1H), 2.84 – 2.69 (m, 1H), 1.98 – 1.65 (m, 5H), 1.60 – 1.49 (m, 1H).[4]

(4,4,5,5,6,6,7,7,8,8,9,9,9-tridecafluoro-2-iodononyl)benzene (15)

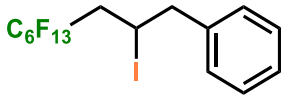

The general procedure was followed using PZM (1.4 mg, 0.5 mol%), $C_6F_{13}I$ (86 µL, 0.4 mmol), allylbenzene (26 µL, 0.2 mmol), TEA (14 µL, 0.1 mmol), MeOH (400 µL), 1 h. Purification by flash column chromatography (gradient eluent from hexane to 20:1 hexane:AcOEt) afforded the title compound (99% yield).
^{1}H NMR (500 MHz, $CHCl_3$): δ 7.57 – 7.15 (m, 5H), 4.48 – 4.40 (m, 1H), 3.40 – 3.15 (m, 2H), 3.03 – 2.71 (m, 2H).[21]

(5,5,6,6,7,7,8,8,9,9,10,10,10-tridecafluoro-3-iododecyl)benzene (16)

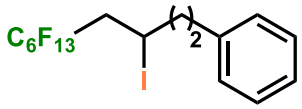

The general procedure was followed using PZM (1.4 mg, 0.5 mol%), $C_6F_{13}I$ (86 µL, 0.4 mmol), 4-phenyl-1-butene (30 µL, 0.2 mmol), TEA (14 µL, 0.1 mmol), MeOH (400 µL), 1 h. Purification by flash column chromatography (gradient eluent from hexane to 20:1 hexane:AcOEt) afforded the title compound (81% yield).
^{1}H NMR (500 MHz, $CHCl_3$): δ 7.30 – 7.13 (m, 5H), 4.27 – 4.20 (m, 1H), 2.98 – 2.64 (m, 4H), 2.15 – 2.04 (m, 2H).[8]

1-methoxy-4-(4,4,5,5,6,6,7,7,8,8,9,9,9-tridecafluoro-2-iodononyl)benzene (17)

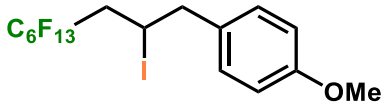

The general procedure was followed using PZM (1.4 mg, 0.5 mol%), $C_6F_{13}I$ (86 µL, 0.4 mmol), 1-methoxy-4-(2-propen-1-yl)benzene (31 µL, 0.2 mmol), TEA (14 µL, 0.1 mmol), MeOH (400 µL), 1 h. Purification by flash column chromatography (gradient eluent from hexane to 20:1 hexane:AcOEt) afforded the title compound (83% yield).
^{1}H NMR (500 MHz, $CHCl_3$): δ 7.10 (d, *J* = 8.6 Hz, 2H), 6.87 (d, *J* = 8.6 Hz, 2H), 4.44 – 4.35 (m, 1H), 3.79 (s, 3H), 3.20 (dd, *J* = 14.8, 6.0 Hz, 1H), 3.12 (dd, *J* = 14.8, 8.8 Hz, 1H), 2.95 – 2.74 (m, 2H).[24]

1-Iodo-2-(tridecafluorohexyl)cyclooctane (18)

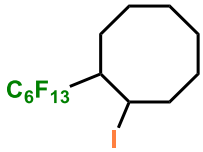

The general procedure was followed using PZM (1.4 mg, 0.5 mol%), $C_6F_{13}I$ (86 µL, 0.4 mmol), cyclooctene (20 µL, 0.2 mmol), TEA (14 µL, 0.1 mmol), MeOH (400 µL), 1 h. Purification by flash column chromatography (gradient eluent from hexane to 20:1 hexane:AcOEt) afforded the title compound (85% yield).
^{1}H NMR (500 MHz, $CHCl_3$): δ 4.61 – 4.59 (m, 1H, major), 4.54 – 4.50 (m, 1H, minor), 2.47 – 2.30 (m, 3H), 2.15 – 1.35 (m, 10H).[8]

(E/Z)-5,5,6,6,7,7,8,8,9,9,10,10,11,11,12,12,12-Heptadecafluoro-3-iodododec-3-en-1-ol (19)

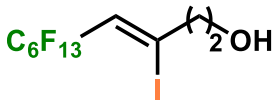

The general procedure was followed using PZM (1.4 mg, 0.5 mol%), $C_6F_{13}I$ (86 µL, 0.4 mmol), 3-butyn-1-ol (15 µL, 0.2 mmol), TEA (14 µL, 0.1 mmol), MeOH (400 µL), 1 h. Purification by flash column chromatography (gradient eluent from hexane to 20:1 hexane:AcOEt) afforded the title compound (*E*/*Z* = 86:13, total 99% yield).
(*E*-isomer) ^{1}H NMR (500 MHz, $CHCl_3$): δ 6.46 (t, *J* = 14.3 Hz, 1H), 3.85 (s, 2H), 2.90 (t, *J* = 6.0 Hz, 2H), 1.44 (br. s, 1H).[9]

1-(3,3,4,4,5,5,6,6,7,7,8,8,9,9,10,10,10-Heptadecafluoro-1-iododec-1-en-1-yl)-4-methoxybenzene (20)

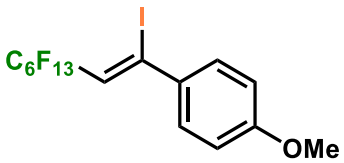

The general procedure was followed using PZM (1.4 mg, 0.5 mol%), $C_6F_{13}I$ (86 µL, 0.4 mmol), 4-ethynylanisole (26 µL, 0.2 mmol), TEA (14 µL, 0.1 mmol), MeOH (400 µL), 1 h. Purification by flash column chromatography (gradient eluent from hexane to 20:1 hexane:AcOEt) afforded the title compound (*E*/*Z* = 94:5, total 99% yield).
(*E*-isomer) ^{1}H NMR (500 MHz, $CHCl_3$): δ 7.24 (d, *J* = 8.6 Hz, 2H), 6.80 (d, *J* = 8.8 Hz, 2H), 6.51 (t, *J* = 13.5 Hz, 1H), 3.77 (s, 3H).[9]

8. References

1. Y. Zhao, R. Wang, Y. Wang, G. Jie and H. Zhou, *Food Chemistry*, 2023, **413**, 135627.
2. C.-J. Wallentin, J. D. Nguyen, P. Finkbeiner and C. R. J. Stephenson, *J. Am. Chem. Soc.*, 2012, **134**, 8875–8884.
3. T. Yajima and M. Ikegami, *Eur. J. Org. Chem.*, 2017, 2126–2129.
4. C. Rosso, G. Filippini, P. G. Cozzi, A. Gualandi and M. Prato, *ChemPhotoChem*, 2019, **3**, 193–197.
5. Z. Liu, C. Li, J. Chen, X. Li, F. Luo, F. Cheng and J.-J. Liu, *Inorg. Chem. Front.*, 2022, **9**, 111–118.
6. G. Filippini, F. Longobardo, L. Forster, A. Criado, G. D. Carmine, L. Nasi, C. D'Agostino, M. Melchionna, P. Fornasiero and M. Prato, *Sci. Adv.*, 2020, **6**, eabc9923.
7. G. Magagnano, A. Gualandi, M. Marchini, L. Mengozzi, P. Ceroni and P. G. Cozzi, *Chem. Commun.*, 2017, **53**, 1591–1594.
8. T. Yajima, M. Murase and Y. Ofuji, *Eur. J. Org. Chem.*, 2020, 3808–3811.
9. T. Zhang, P. Wang, Z. Gao, Y. An, C. He and C. Duan, *RSC Adv.*, 2018, **8**, 32610–32620.
10. X. Liu, Z. Guo, Y. Che, R. Bai, Y. Chi, C. Guo and H. Xing, *ACS Appl. Mater. Interfaces*, 2021, **13**, 34114–34123.
11. A. Gualandi, G. Rodeghiero, E. D. Rocca, F. Bertoni, M. Marchini, R. Perciaccante, T. P. Jansen, P. Ceroni and P. G. Cozzi, *Chem. Commun.*, 2018, **54**, 10044–10047.
12. E. Arceo, E. Montroni and P. Melchiorre, *Angew. Chem. Int. Ed.*, 2014, **53**, 12064–12068.
13. C. Rosso, G. Filippini and M. Prato, *Chem. Eur. J.*, 2019, **25**, 16032–16036.
14. Z. Zhu, H. Huang, L. Liu, F. Chen, N. Tian, Y. Zhang and H. Yu, *Angew. Chem. Int. Ed.*, 2022, **61**, e202203519.
15. Y. Hu, X. Hao, Z. Cui, J. Zhou, S. Chu, Y. Wang and Z. Zou, *Appl. Catal. B*, 2020, **260**, 118131.
16. M. A. Cismesia and T. P. Yoon, *Chem. Sci.*, 2015, **6**, 5426–5434.
17. E. Fernandez, J. M. Figuera and A. Tobar, *J. Photochem.*, 1979, **11**, 69–71.
18. W. D. Bowman and J. N. Demas, *J. Phys. Chem. C*, 1976, **20**, 2434–2435.
19. C. G. Hatchard and C. A. Parker, *Proc. Roy. Soc.*, 1956, **A235**, 518–536.
20. C. A. Parker, *Proc. Roy. Soc.*, 1953, 104–115.
21. T. Tasnim, C. Ryan, M. L. Christensen, C. J. Fennell and S. P. Pitre, *Org. Lett.*, 2022, **24**, 446–450.
22. J.-Y. Sun, J. Li, X.-L. Qiu and F.-L. Qing, *Journal of Fluorine Chemistry*, 2005, **126**, 1425–1431.
23. F. Longobardo, G. Gentile, A. Criado, A. Actis, S. Colussi, V. Dal Santo, M. Chiesa, G. Filippini, P. Fornasiero, M. Prato and M. Melchionna, *Mater Chem Front.*, 2021, ***5***, 7267–7275.
24. T. Mao, M.-J. Ma, L. Zhao, D.-P. Xue, Y. Yu, J. Gu and C.-Y. He, *Chem. Comm.*, 2020, **56**, 1815–1818.
25. D. T. Anh, H. Blancou and A. Commeyras, *Journal of Fluorine Chemistry*, 1999, **96**, 167–174.